East European Journal of Physics. 3. 546-554 (2023)
DOI:10.26565/2312-4334-2023-3-64 ISSN 2312-4334

ENHANCEMENTS OF STRUCTURAL AND OPTICAL PROPERTIES OF MgO: SnO_2 NANOSTRUCTURE FILMS[†]

R.H. Ayoub[a], Muhammad H. Al-Timimi[a]*, M.Z. Abdullah[b]
[a]*Department of Physics, College of Science, University of Diyala, Iraq*
[b]*Materials Research Directorate, Ministry of Science and Technology, Iraq*
**Corresponding Author e-mail: muhammadtimimi@yahoo.com*
Received July 10, 2023; revised August 3, 2023; accepted August 5, 2023

This study uses the chemical precipitation method to investigate the structural and optical properties of MgO:SnO_2 nanoparticles. The thin films were deposited by the spin coating technique on glass substrates. X-ray diffraction analysis proved the crystalline structure of prepared thin films, with the peaks corresponding to the (110), (101), (200), (211), and (220) planes, with the tetragonal SnO_2 crystal structure. Fourier transforms infrared (FTIR), and scanning electron microscope (SEM) are used to characterize the functional groups, shape, and dimensions of synthesized metal oxide nanoparticles. The optical properties of the films were studied by UV-Vis spectroscopy. The bandgap energy was estimated to be in the range of (3.9-3.4 eV). The refractive index and extinction coefficient of the films were also determined, and the results indicated that the films had good transparency in the visible region. The study concludes that MgO:SnO_2 thin films obtained by the spin coating technique have potential applications in optoelectronics and gas sensors.
Keywords: *MgO:SnO_2 films; Spin coating technique; Precipitation method; Structure; Optical properties*
PACS: 73.20.At, 78.20.-e, 77.55.+f

INTRODUCTION

MgO:SnO_2 nanoparticles are composite particles consisting of magnesium oxide (MgO) and tin dioxide (SnO_2) in the form of nanoparticles. These nanoparticles can be synthesized using various methods, including sol-gel [1,2], co-precipitation [3], and hydrothermal methods [4]. MgO:SnO_2 nanoparticles have attracted significant attention due to their unique properties, such as high surface area, high reactivity, and good stability [5]. These properties make them suitable for various applications, including gas sensing, catalysis, energy storage, and biomedical applications. One of the main applications of MgO:SnO_2 nanoparticles is in gas sensing [6]. These nanoparticles have been shown to exhibit excellent sensitivity and selectivity towards various gases, such as CO, NO_2, and H_2 [7]. The high surface area of the nanoparticles provides a large surface area for gas adsorption, while the SnO_2 component provides a high catalytic activity for gas oxidation. In addition, MgO:SnO_2 nanoparticles have been investigated for their catalytic activity in various reactions, such as CO oxidation, methanol synthesis, and photocatalysis [8]. The unique properties of the nanoparticles, such as their size and composition, can be tuned to optimize their catalytic activity [9]. MgO:SnO_2 nanoparticles also show promise in energy storage applications, such as in lithium-ion batteries [10,11]. The nanoparticles can be used as anode materials due to their high lithium-ion storage capacity and good cycling stability. Furthermore, MgO:SnO_2 nanoparticles have potential biomedical applications, such as in drug delivery and cancer therapy [12]. The nanoparticles can be functionalized with various ligands and drugs to target specific cells or tissues, and their high stability and biocompatibility make them suitable for in vivo applications. Overall, MgO:SnO_2 nanoparticles have a wide range of potential applications due to their unique properties and can be synthesized using various methods [13,14].

Spin coating is a popular method for depositing thin films, especially for research and development purposes, due to its ease of use, low cost, and compatibility with various materials. In this method, a liquid solution containing the desired precursor materials is first applied onto a spinning substrate, such as a glass or silicon wafer [15,16]. The centrifugal force generated by the spinning causes the solution to spread uniformly across the substrate and evaporate, leaving behind a thin film on the surface [17]. MgO:SnO_2 thin films obtained by spin coating have potential applications in various fields, including optoelectronics [18], and gas sensors [19]. The properties of the thin films, such as their thickness, composition, and morphology, can be tuned by adjusting the concentration and ratio of the precursor materials in the solution and the spin-coating parameters, such as spin speed, spin time, and temperature [20].

The study aimed to characterize MgO:SnO_2 by Co-Precipitation method and prepares thin films by spin coating and study the structural properties of the nanoparticles using XRD analysis, determine the surface morphology using SEM, investigate the optical properties of the thin films using UV-Vis spectroscopy, and study the properties of MgO:SnO_2 thin films obtained by spin coating.

EXPERIMENTAL PART

1. **Materials**. Magnesium chloride $MgCl_{2.6}H_2O$, Tin chloride $SnCl_{2.2}H_2O$, Ammonium hydroxide solution, Deionized water

[†] ***Cite as:*** R.H. Ayoub, M.H. Al-Timimi, M.Z. Abdullah, East Eur. J. Phys. 3, 546 (2023), https://doi.org/10.26565/2312-4334-2023-3-64

2. **Equipment.** Magnetic stirrer (China-Wincom Co. Ltd.), Glass beaker, Centrifuge (China-Wincom Co. Ltd.), Drying oven (Germany -Memmert UE 500 Lab Oven), Spin coating device (Britain-Ossila co.).

3. **Procedure.** Weigh out the desired amounts of Magnesium chloride and tin (IV) chloride and dissolve them in deionized water separately, Slowly add the Magnesium chloride solution to the tin chloride solution while stirring continuously with a magnetic stirrer with percentages MgO_{1-x}: SnO_2 x (x=0.2,0.3,0.4,0.5), adding Ammonium hydroxide solution to the mixture until the pH reaches around 9, The mixture will turn white and a precipitate will form, Continue stirring the mixture for another 2-3 hours to ensure complete precipitation of the nanoparticles, Centrifuge the mixture at a high speed (around 10,000 rpm) for 15-20 minutes to collect the precipitate, Washing the precipitate with deionized water to remove any impurities and residual reactants. Finally Drying the nanoparticles in an oven at a low temperature (around 80°C) for several hours until all the solvent is evaporated and the nanoparticles are fully dried and Calcination at 800°C.

The MgO_{1-x}: SnO_2 x (x=0.2,0.3,0.4,0.5), thin films were prepared by the addition (the MgO_{1-x}: SnO_2 nanoparticles dissolved in ethylene glycol with a mass ratio (0.1:10) at room temperature), the MgO, SnO_2, and MgO:SnO_2 concentration was 0.1 g. Glass substrates were successively cleaned with acetone, ethanol, and deionized water. MgO, SnO_2, and MgO:SnO_2 thin films were deposited on the glass substrates by spin coating at room temperature with a rate of 2000 rpm for 30 s, the spin-coating step, the films were heated on a hot plate at 30-50 °C in the air for 10 min to remove organic contaminations.

RESULTS AND DISCUSSION

The X-ray diffraction (XRD) test was carried out on prepared samples to determine the crystal structure type and the crystalline size using an x-ray (Shimadzu-6000) diffractometer, with wavelength (λ=1.54060°A) and voltage (40 KV). Fig. 1 shows the obtained XRD patterns of prepared samples. The detected peaks at (2Θ = 36.98°, 42.97°, 62.39°, 74.8° and 78.75°) of the crystalline planes (111), (002), (022), (113) , and (222) demonstrated the formation of cubic MgO structure, space group (Fm-3m no. 225), with lattice parameters (a=b=c= 4.2060 A°) and (α=β=γ=90°), which well agreed with the standard data (JCPDS 98-016-9450). While the peaks at (2Θ = 26.59°, 33.89°, 37.96°, 51.79°, 54.77°, 57.85°, 61.9°, 64.77°, 65.99°, 71.31° and 78.74°) of the planes (110), (011), (020), (121), (220), (002), (130), (112), (031), (002) , and (231) attributed to the Cassiterite tetragonal SnO_2 structure, space group (P42/mnm no.136), with lattice parameters (a = b = 4.7360 Å and c = 3.1850 Å) and (α=β=γ=90°) corresponded to the standard data (JCPDS 98-003-9173). As shown in Fig. 1(a,b).

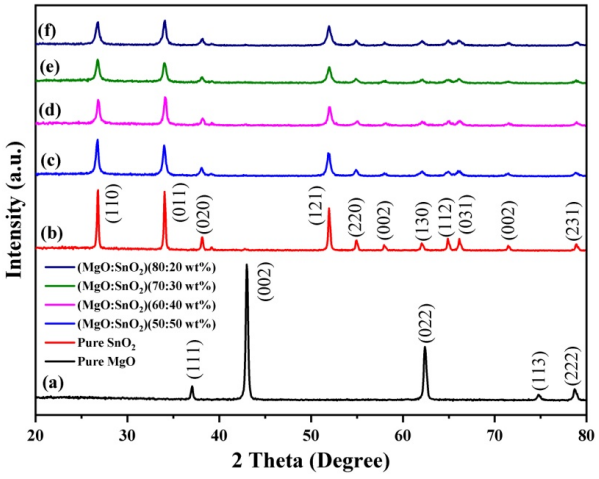

Figure 1. XRD patterns of synthesized samples

The XRD results revealed the highly pure crystalline structure of the synthesized MgO, SnO_2, and MgO:SnO_2 nanoparticles, where there are no impurities peaks appearing in the obtained XRD patterns. After doping with MgO, observed that the crystal structure of SnO_2 has not changed in all MgO ratios (50, 60, 70 and 80 wt. %), suggesting that the Mg ions were incorporated within the SnO_2 crystalline lattice, cassiterite tetragonal structure of pure MgO:SnO nanoparticles with space group (P42/mnm no.136) obtained. The XRD patterns demonstrated that the peaks intensity of pure SnO_2 decreased after the doping process, while the full-width half maximum value (FWHM) increased, which can be attributed to the SnO_2 crystalline growth decreased by Mg ions doping as shown in Fig. 1(c,d,e,f), this is due to the smaller diameter of Mg ions (0.067 nm) compared to the tin ions (0.071 nm) [21, 22].

The crystalline sizes of the pure MgO, SnO_2 and different ratio (50, 60, 70 and 80 wt. %) of Mg ions doped SnO_2 were calculated depending on the highest XRD peak using Scherrer's equation [23], to be (24.5 nm), (35.42 nm), (19.89 nm), (18.97 nm), (14.55 nm), (14.11 nm) respectively. The results indicated a clear decrease in crystalline size with the doping Mg ions ratio, as a result of the difference in the ion size of Sn and Mg ions [24].

The samples have been investigated using the FTIR test to determine the functional groups within the prepared materials. The FTIR spectra of MgO, SnO_2, and MgO:SnO_2 powder in the wavenumber range (500-4000 cm^{-1}) are shown in Fig. 8. The stretching and bending vibrations of metal-oxygen (MgO and SnO_2) bonds detected at the range

(1500-900 cm^{-1}), spectroscopic evidence points to the presence of Sn-O and Mg-O vibrations bonds at the broad peak centered around (616 cm^{-1}) [23].

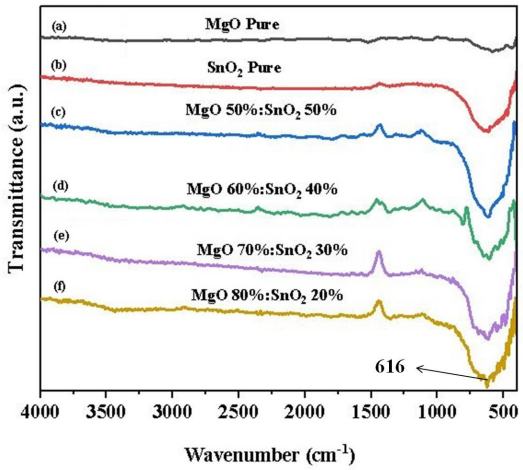

Figure 2. FTIR curve of synthesized samples

Figure 3 presents the results of Scanning Electronic Microscopy images and particle size distributions of prepared samples. The synthesized nanoparticles exhibited a semi-spherical nanoparticle of all samples, as shown in Fig. 3 (a,b,c,d,e,f). The results revealed that the average particle size of pure MgO is about (117.93 nm), while the smaller average particle size (90.07 mn) for pure SnO_2 nanoparticles. As presented in Fig. 3(a, b), the SEM images clearly show that the SnO_2 nanoparticles are approximately identical in size. Fig. 3(c,d,e,f) showed the morphology of MgO nanoparticles doped with different ratios of SnO_2. The SEM images revealed the agglomeration of doped nanoparticles with semi-spherical shapes, and the MgO:SnO_2 nanoparticles gathered as clusters. Finally, the SEM image demonstrated that the average particle size significantly decreased with the doping with the SnO_2, to be (48.71 nm), (48.5 nm), (50.05 nm) and (50.3 nm) of the SnO_2 ratio (50, 60, 70 and 80 wt. %) respectively, which can be attributed to the smaller ionic radius of Sn ions compared with Mg ions [24, 25].

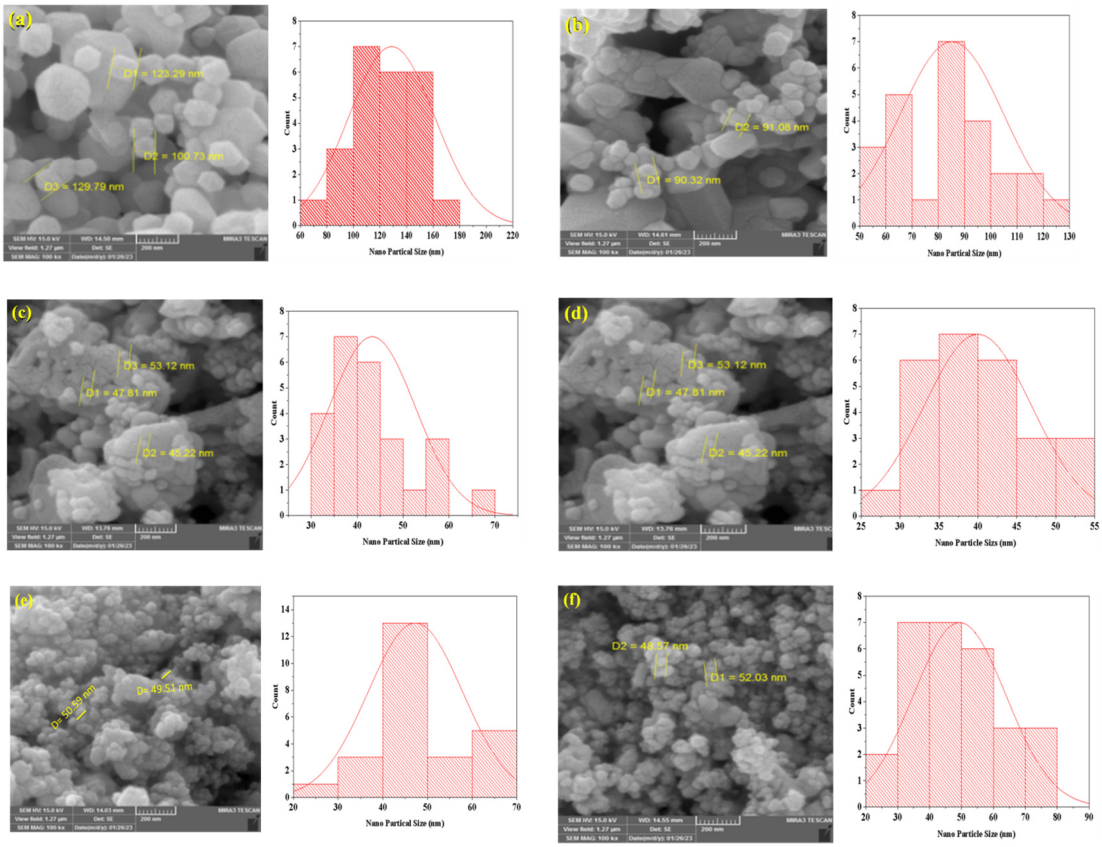

Figure 3. SEM images and particle size distribution of prepared samples (a) pure MgO, (b) pure SnO_2, (c) $MgO_{(0.5)}$: $SnO_{2(0.5)}$, (d) $MgO_{(0.6)}$: $SnO_{2(0.4)}$, (e) MgO $_{(0.7)}$: $SnO_{2(0.3)}$, (f) $MgO_{(0.8)}$: $SnO_{2(0.2)}$

UV-Vis absorption spectroscopy is a useful technique to investigate the optical properties of prepared films. The films were deposited on glass substrates using the spin coating technique. Optical measurements are conducted in the range of 200-1200 nm to determine the optical parameters. The optical absorption and transmission spectra of the MgO nanoparticles revealed a change in the band gap transition as the concentration of SnO_2 is increased, with a higher percentage of dopant, there is a small shift toward the longer wavelength region. The sharp increase in the spectra at the absorption edge demonstrates highly crystalline nanoparticles with few surface defects within the films [26, 27]. Transmittance and reflectance were calculated separately, the transmittance spectra of the films are plotted as a function of the wavelength of incident light of all MgO:SnO_2 samples. The transmittance spectra is directly related to the concentration of SnO_2, It is worth noting that the maximum value of reflectance occurs at a wavelength of 350 nm and decreases with the visible wavelength as shown in Fig. 4.

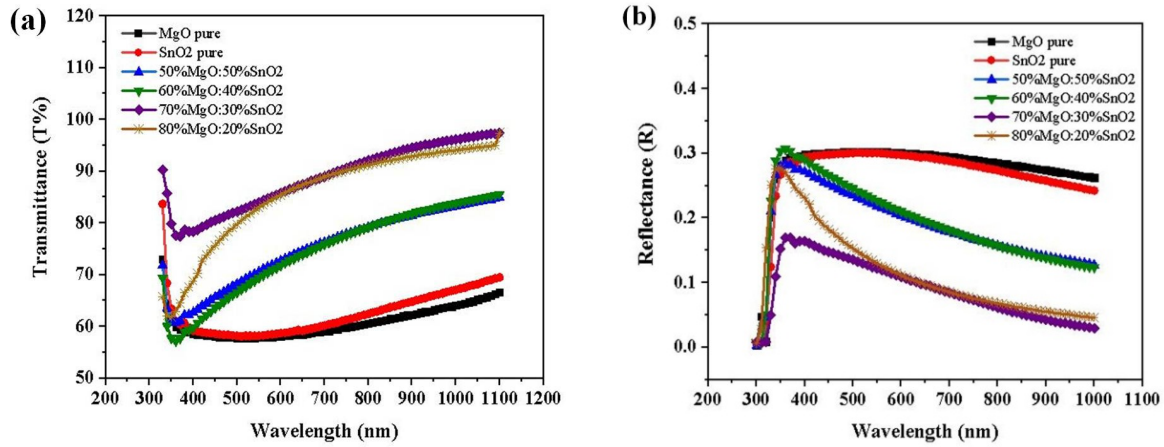

Figure 4. (a) Transmittance and (b) reflectance spectra of prepared MgO:SnO_2 films

The absorption coefficient (α) was determined using the following equation, which was derived from the absorptance spectrum [28]:

$$\alpha = 2.303\frac{A}{t} \quad (1)$$

The absorbance (A) is used in the calculation of the absorption coefficient (α), As depicted in Fig. 5, the absorption coefficient (α) decreases as the concentration of MgO increases. This is attributed to the increase in the energy gap that occurs with higher concentrations of MgO.

The absorption coefficient (α) describes how well a material can absorb light at a particular wavelength. In the case of MgO: SnO_2 film, an increase in the concentration of MgO leads to a widening of the bandgap [29], which is the energy range where electrons are not available to absorb photons [30,31]. This means that fewer photons are absorbed by the film, resulting in a decrease in the absorption coefficient (α). Therefore, as the concentration of MgO increases, the film becomes less efficient in absorbing light, causing a decrease in the absorption coefficient, which agreed with the results [32, 33].

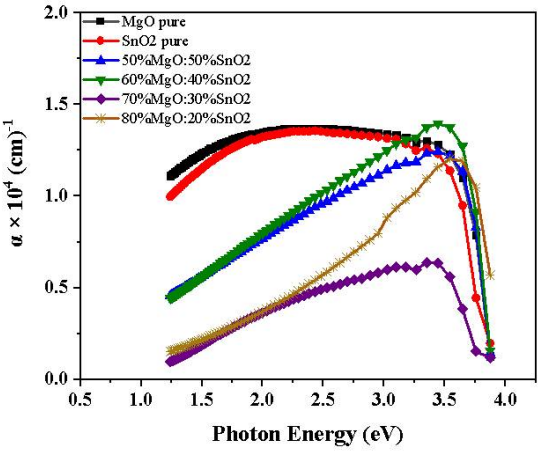

Figure 5. Absorption coefficient (α) of prepared MgO:SnO_2 films

Fig. 6 shows the bandgap energy of pure MgO film, pure SnO_2 film, and MgO:SnO_2 films. The bandgap energy of the sample can be determined using the formula [34,35] :

$$\alpha h\vartheta = C(h\vartheta - E_g)^{1/2} \quad (2)$$

Assuming a constant value (C) for the absorption coefficient (α), the bandgap energies of MgO: SnO_2 nanoparticles were approximately 3.9 eV, while those of tin oxides were around 3.6 eV. The bandgap energy of pure MgO was approximately 3.5 eV. These values were obtained for (MgO) (SnO_2) (MgO: SnO_2) films. When these two materials are combined in the form of a composite film, their bandgap energies are affected by several factors, including the concentration of the materials and the degree of crystallinity [36]. The addition of SnO_2 to MgO can cause the bandgap energy to decrease, as observed in the case of the MgO:SnO_2 films. This is due to the change in the electronic structure of the composite film, which arises from the interaction between the two materials [37,38].

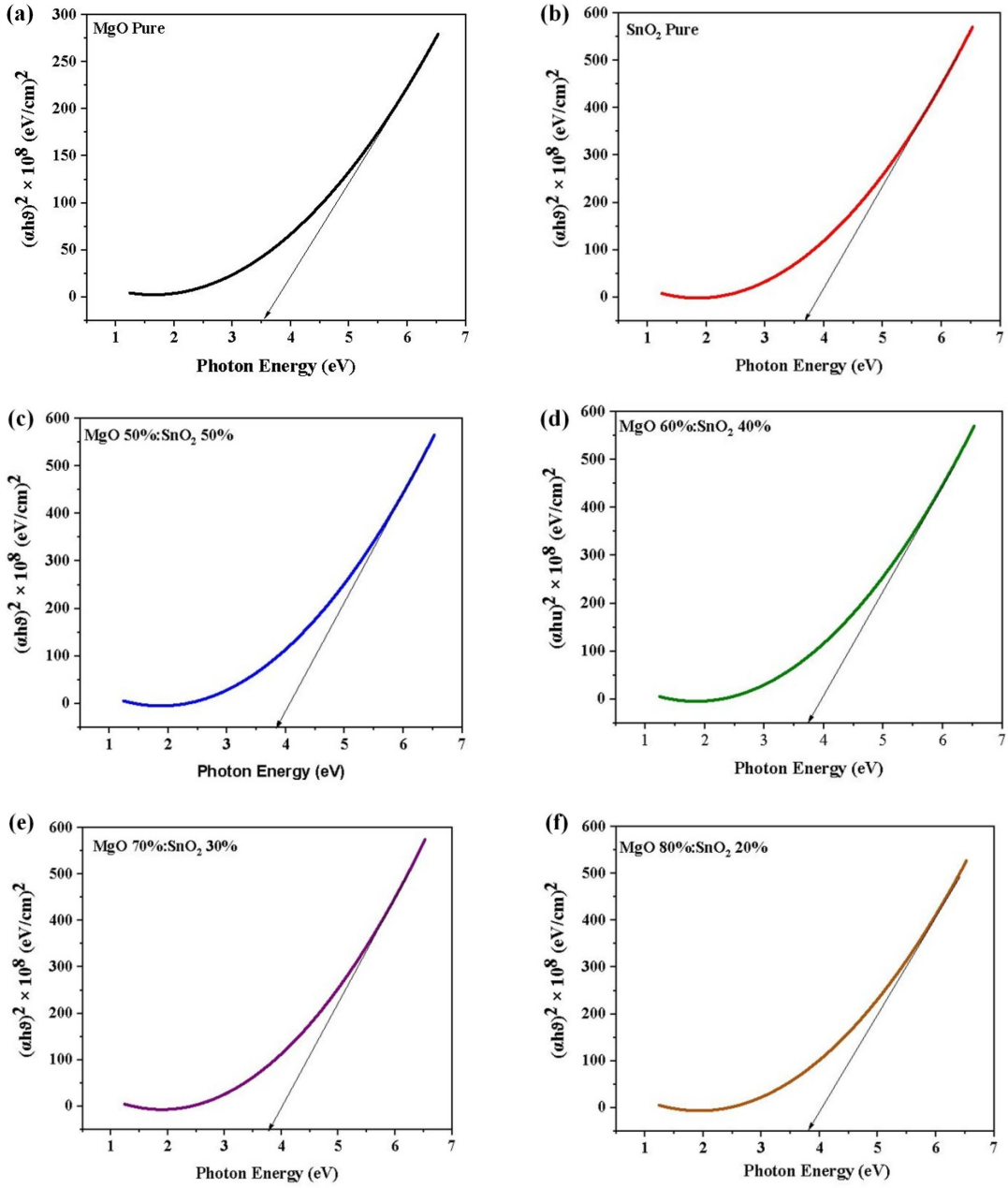

Figure 6. Energy band gap curves of prepared samples (a) pure MgO, (b) pure SnO_2, (c) 80%MgO:20%SnO_2, (d) 80%MgO:20%SnO_2, (e) 80%MgO:20%SnO_2, (f) 80%MgO:20%SnO_2

By using relation (3), the refractive index of both pure MgO, SnO_2 films, and (MgO: SnO_2) films has been calculated [39].

$$n_o = \frac{1+R}{1-R} + \left(\frac{4R}{(1-R)^2} - k_o\right)^{1/2} \quad (3)$$

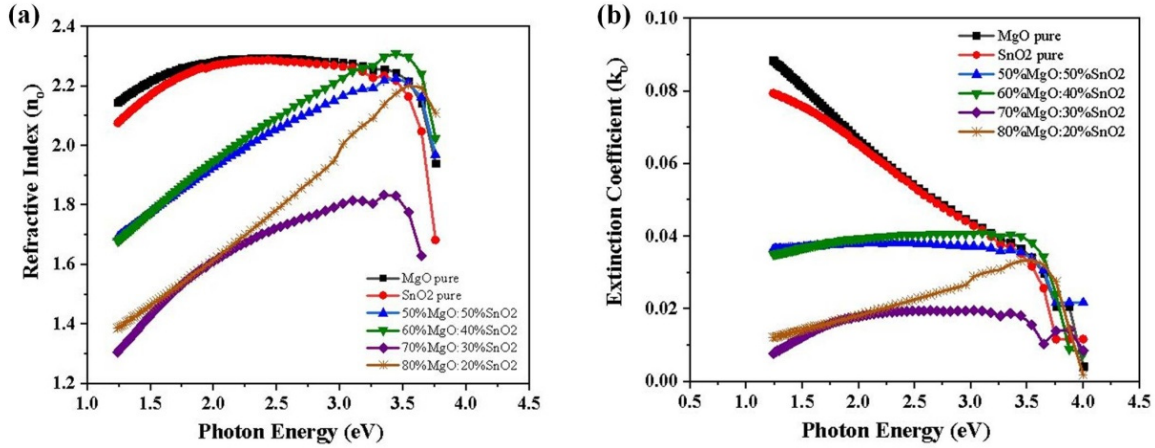

Figure 7. (a) Refractive index and (b) extinction coefficient curves of prepared films

The absorption spectra can be used to calculate the extinction coefficient from the equation (4) [40,41]:

$$k_o = \frac{\alpha\lambda}{4\pi} \tag{4}$$

The fundamental dielectric constant is shown in Figure 8. We can see that the value of 60% MgO:40%SnO_2 is maximum (5) at the photon Energy (3.5eV), while the value of 70% MgO:30% SnO_2 decreases to (3) at the wavelength. (3.5eV). The values of (n_o) and (k_o) are connected to the real (ε_r) and imaginary (ε_i) components of the dielectric constant, The formulae (5) and (6) were utilized to calculate the values of (ε_r) and (ε_i), respectively [42, 43]:

$$\varepsilon_r = n_\circ^2 - k_\circ^2 \tag{5}$$

$$\varepsilon_i = 2n_\circ k_\circ \tag{6}$$

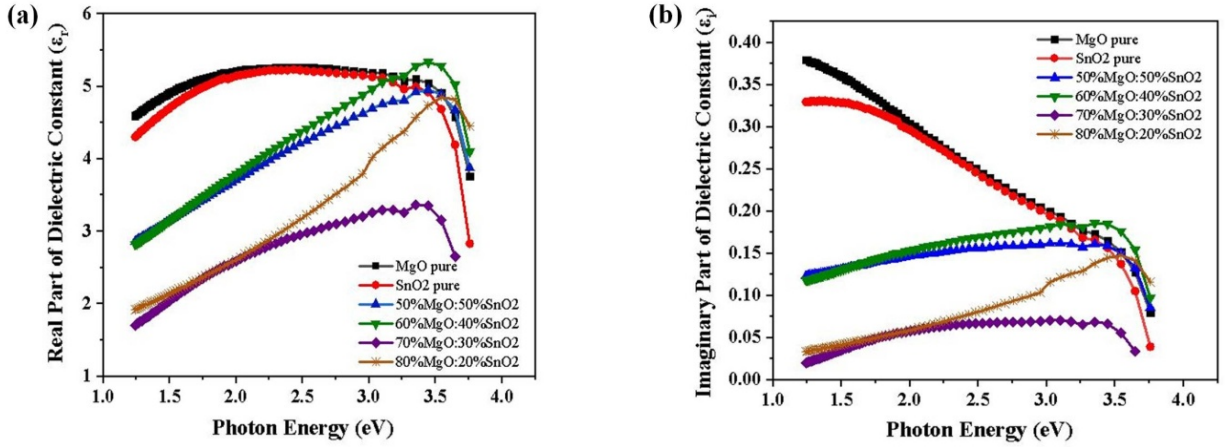

Figure 8. (a) Real part and (b) imaginary part of dielectric constant curves of prepared films

Figure 8(a) presents the real dielectric constant with the highest value of 5.21 observed at a photon energy of 3.5 eV of the 60%MgO:40%SnO_2 film, while the lowest value of 3.18 is observed at the photon energy of 3.25 eV of the 70%MgO:30%SnO_2 film. Figure 8(b) illustrates the imaginary dielectric constant, with the highest value of 0.384 observed at a photon energy of 1.3 eV for the Pure MgO film, and the lowest value of 0.023 observed at the photon energy of 0.384 eV for the 70%MgO:30%SnO_2 film. In general, both the real and imaginary dielectric constants exhibited a change in the behavior with an increase in the doping ratio [44,45].

CONCLUSIONS

The co-precipitation method proved successful in synthesizing MgO, SnO_2, and MgO:SnO_2 nanoparticles with distinct characteristics. X-ray diffraction analysis revealed an average crystallite size of 33 nm, while particle size analyzer results indicated an average particle size of 22 nm. The samples exhibited different crystal structures, with MgO having a cubic structure, SnO_2 nanoparticles showing a tetragonal structure, and MgO:SnO_2 displaying a tetragonal structure as well. SEM images provided further evidence of spherical and aggregated particles with a granular crystalline structure. The nanoparticles were further characterized using UV-Vis spectroscopy. It was observed

that increasing the SnO_2 concentration doping led to enhanced transmittance in the MgO:SnO_2 films. Moreover, the energy band gap increased with higher SnO_2 concentration, the refractive index, extinction coefficient, and real and imaginary dielectric constant components of the material also increased with rising SnO_2 concentration. The synthesized nanoparticles have potential applications in various fields, such as optoelectronics, and sensors.

ORCID

R.H. Ayoub, https://orcid.org/0009-0002-6590-8258; **Muhammad H. Al-Timimi**, https://orcid.org/0000-0002-9828-6945
M.Z. Abdullah, https://orcid.org/0000-0002-4087-7830

REFERENCES

[1] J. Xiong, Y. Xue, Y.-D. Xia, F. Zhang, Y.-X. Zhang, L.-H. Li, X.-H. Zhao, and B.-W. Tao, "Fabrication of long-length ion beam-assisted deposited MgO templates for YBCO coated conductors," Rare Met. **32**, 574-578 (2013). https://doi.org/10.1007/s12598-013-0164-4

[2] S. Stankic, M. Sterrer, P. Hofmann, J. Bernardi, O. Diwald, and E. Knozinger, "Novel optical surface properties of Ca^{2+}-doped MgO nanocrystals," Nano Lett. **5**, 1889-1893 (2005). https://doi.org/10.1021/nl0511418

[3] M.H. Al-Timimi, W.H. Albanda, and M.Z. Abdullah, "Influence of Thickness on Some Physical Characterization for Nanostructured MgO Thin Films," East European Journal of Physics, (2), 173-181 (2023). https://periodicals.karazin.ua/eejp/article/view/21350

[4] Y. Cai, D. Wu, X. Zhu, W. Wang, F. Tan, J. Chen, X. Qiao, and X. Qiu, "Sol-gel preparation of Ag-doped MgO nanoparticles with high efficiency for bacterial inactivation," Ceram. Int. **43**, 1066-1072 (2017). https://doi.org/10.1016/j.ceramint.2016.10.041

[5] M.Z. Abdullah, M.H. Al-Timimi, W.H. Albanda, M. Dumitru, A.E. Balan, Ceaus, et al., "Structural and Electrochemical Properties of P3-$Na_{0.67}Mn_{0.3}Co_{0.7}O_2$ Nanostructures Prepared by Citric-Urea Self-Combustion Route as Cathode for Sodium Ion Battery," Digest Journal of Nanomaterials and Biostructures, **14**(4), 1179-1193 (2019). https://chalcogen.ro/1179_AbdullahMZ.pdf

[6] A.M.E. Raj, L. Nehru, M. Jayachandran, and C. Sanjeeviraja, "Spray pyrolysis deposition and characterization of highly (100) oriented magnesium oxide thin films," Crystal Research and Technology, J. Exp. Indust. Crystallogr. **42**, 867-875 (2007). https://doi.org/10.1002/crat.200710918

[7] J. Lee, T. Jeong, S. Yu, S. Jin, J. Heo, W. Yi, and J. Kim, "Secondary electron emission of MgO thin layers prepared by the spin coating method," J. Vac. Sci. Technol. B: Microelectr. Nanometer Struct. Proc. Measure. Phenomena, **19**, 1366-1369 (2001). https://doi.org/10.1116/1.1383079

[8] I.M.I. Moustafa, and M.R. Abdelhamid, "Synthesis of MgO-ZrO_2 mixed nanoparticles via diferent precursors: identifcation of their destructive action for organic pollutants," J. Chem. Eng. Process. Technol. **9**(1), 372 (2018). https://doi.org/10.4172/2157-7048.1000372

[9] M. Kiaei, Y.R. Moghdam, B. Kord, and A. Samariha, "The effect of nano-MgO on the mechanical and fammability properties of hybrid nano composites from wood four-polyethylene," Maderas. Ciencia y Tecnología, **19(**4), 471-480 (2017). http://dx.doi.org/10.4067/S0718-221X2017005000701

[10] H.M. Hussein, and M.H. Al-Timimi, "Preparation and Study Some Physical Properties of (CMC/PAA: MgO) Nano Composites," Eurasian Journal of Physics, Chemistry and Mathematics, **8**, 47-55 (2022). https://www.geniusjournals.org/index.php/ejpcm/article/view/1944

[11] Abdullah, M. Z., Hasan, H. M., Al-Timimi, M. H., Albanda, W. H., Alhussainy, M. K., & Dumitru, M. "Preparation And Characterization Of Carbon Doped Lithium Iron Phosphate Composite As Cathode For Rechargable Battery" . Journal of Ovonic Research Vol, 15(3), 199-204 (2019). https://chalcogen.ro/199_AbdullahMZ.pdf

[12] I.-C. Ho, Y. Xu, and J. D. Mackenzie, "Electrical and Optical Properties of MgO Thin Film Prepared by Sol-Gel Technique," Journal of Sol-Gel Science and Technology, **9**, 295-301 (1997). https://doi.org/10.1023/A:1018315529408

[13] A.M.E. Raj, M. Jayachandran, and C. Sanjeevijaya, "Fabrication techniques and material properties of dielectric MgO thin films- A status review," CIRP Journal of Manufacturing Science and Technology, **2**(2), 92-113 (2010). https://doi.org/10.1016/j.cirpj.2010.02.003

[14] A.D. Bhagwat, S.S. Sawant, B.G. Ankamwar, and C.M. Mahajan, "Synthesis of nanostructured tin oxide (SnO_2) powders and thin flmsby sol-gel method," J. Nano Electron. Phys. **7**(4), 04037 (2015). https://jnep.sumdu.edu.ua/en/component/content/full_article/1658

[15] A. Mariam, V.S. Vidhya, S. Sivaranjani, M. Bououdina, R. Perumalsamy, and M. Jayachandran, "Synthesis and characterizations of SnO_2 nanoparticles," J. Nanoelectron. Optoelectron. **8**, 273-280 (2013). https://doi.org/10.1166/jno.2013.1471

[16] S. Vishniakou, R. Chen, Y.G. Ro, C.J. Brennan, C. Levy, E.T. Yu, and S.A. Dayeh, "Improved performance of zinc oxide thin flm transistor pressure sensors and a demonstration of a commercial chip compatibility with the new force sensing technology," Adv. Mater. Technol. **3**(3), 1700279 (2018). https://doi.org/10.1002/admt.201700279

[17] C.I. Priyadharsini, M. Sumathi, A. Prakasam, P.M. Anbarasan, R. Sathiyapriya, and V. Aroulmoji, "Effect of Mg doping on structural and optical properties of SnO_2 nanoparticles by chemical co-precipitation method," Int. J. Adv. Sci. Eng. **3**, 428-434 (2017). https://doi.org/10.1016/j.phpro.2012.03.077

[18] B. Bendahmane, M. Tomić, N.E.H. Touidjen, I. Gracia, S. Vallejos, and F. Mansour, "Influence of Mg doping levels on the sensing properties of SnO_2 films," Sensors, **20**(7), 2158 (2020). https://doi.org/10.3390/s20072158

[19] K. Sujatha, T. Seethalakshmi, and O.L. Shanmugasundaram, "Synthesis, characterization of nano tin oxide via co-precipitation method," Nanotechnology Research and Practice, **11**(3), 98-105 (2016). https://doi.org/10.13187/nrp.2016.11.98

[20] T.S. Vijayakumar, S. Karthikeyeni, S. Vasanth, A. Ganesh, G. Bupesh, R. Ramesh, M. Manimegalai, and P. Subramanian, "Synthesis of silver-doped zinc oxide nanocomposite by pulse mode ultrasonication and its characterization studies," J. Nanosci. **2013**, Article ID 785064 (2013). https://doi.org/10.1155/2013/785064

[21] P.S. Shajira, M.J. Bushiri, B.B. Nair, and V.G. Prabhu, "Energy band structure investigation of blue and green light emitting Mg doped SnO_2 nanostructures synthesized by combustion method," Journal of Luminescence, **145**, 425-429 (2014). https://doi.org/10.1016/j.jlumin.2013.07.073

[22] S. Vadivel, and G. Rajarajan, "Effect of Mg doping on structural, optical and photocatalytic activity of SnO_2 nanostructure thin films," Journal of Materials Science: Materials in Electronics, **26**, 3155-3162 (2015). https://doi.org/10.1007/s10854-015-2811-z

[23] Md.M. Rashad, A. Ismail, I. Osama, I.A. Ibrahim, and A-H T. Kandil, "Photocatalytic decomposition of dyes using ZnO doped SnO_2 nanoparticles prepared by solvothermal method," Arab. J. Chem. **7**, 71-77 (2014). https://doi.org/10.1016/j.arabjc.2013.08.016

[24] L.J.Q. Maia, C.R. Ferrari, V.R. Mastelaro, A.C. Hernandez, and A. Ibanez, "Raman and photoluminescence of Er^{3+}-doped SnO_2 obtained via the sol-gel technique from solutions with distinct pH," Solid State Sci. **10**, 1935 (2008).

[25] Y.C. Liang, and Y. Chao, "Enhancement of acetone gas-sensing responses of tapered WO3 nanorods through sputtering coating with a thin SnO_2 coverage layer," Nanomaterials, **9**(6), 864 (2019). https://doi.org/10.3390/nano9060864

[26] Mohammed, A. A., Ahmed, A. R., & Al-Timimi, M. H. Structural, " Optical and Thermal Properties of (PEG/PAA: MnO2) Nano Composites". Technium BioChemMed, 3(2), 107-119(2022). https://doi.org/10.47577/biochemmed.v3i2.7116

[27] W.A. Aelawi, S. Alptekin, and M.H. Al-Timimi, "Structural, optical, and electrical properties of nanocrystalline CdS_{1-x} CuS_x thin films," Indian Journal of Physics, 1-8 (2023). https://doi.org/10.1007/s12648-023-02736-6

[28] S. Balamurugan, J. Jainshaa, and S.A. Ashika, "Comparison of the synthesis of s, p, d, and f block simple oxides of MgO, SnO_2, NiO, and CeO_2 nanostructured materials," Results in Chemistry, **5**, 100864 (2023). https://doi.org/10.1016/j.rechem.2023.100864

[29] A. Velmurugan, and A.R. Warrier, "Production of biodiesel from waste cooking oil using mesoporous MgO-SnO_2 nanocomposite," Journal of Engineering and Applied Science, **69**(1), 92 (2022). https://doi.org/10.1186/s44147-022-00143-y

[30] S. S. Mirtalebi, H. Almasi, & M. A. Khaledabad, "Physical, morphological, antimicrobial and release properties of novel MgO-bacterial cellulose nanohybrids prepared by in-situ and ex-situ methods," International journal of biological macromolecules, **128**, 848-857 (2019). https://doi.org/10.1016/j.ijbiomac.2019.02.007

[31] H.S. Al-Rikabi, M.H. Al-Timimi, and W.H. Albanda, "Morphological and optical properties of $MgO_{1-x}ZnS_x$ thin films," Digest Journal of Nanomaterials & Biostructures (DJNB), **17**(3), (2022). https://doi.org/10.15251/DJNB.2022.173.889

[32] M.H. Saeed, M.H. Al-Timimi, and O.A.A. Hussein, "Structural, morphological and optical characterization of nanocrystalline WO_3 thin films," Digest Journal of Nanomaterials and Biostructures, **16**(2), 563-569 (2021). https://chalcogen.ro/563_SaeedMH.pdf

[33] H. Si, C. Xu, Y. Ou, G. Zhang, W. Fan, Z. Xiong, A. Kausar, et al., "Dual-passivation of ionic defects for highly crystalline perovskite," Nano Energy, **68**, 104320 (2020). https://doi.org/10.1016/j.nanoen.2019.104320

[34] A.T. Abood, O.A.A. Hussein, M.H. Al-Timimi, M.Z. Abdullah, H.M.S. Al Aani, and W.H. Albanda, "Structural and optical properties of nanocrystalline SnO_2 thin films growth by electron beam evaporation," AIP Conference Proceedings, **2213**(1), 020036 (2020). https://doi.org/10.1063/5.0000454

[35] J. Dagar, S. Castro-Hermosa, G. Lucarelli, F. Cacialli, and T.M. Brown, "Highly efficient perovskite solar cells for light harvesting under indoor illumination via solution processed SnO_2/MgO composite electron transport layers," Nano Energy, **49**, 290-299 (2018). https://doi.org/10.1016/j.nanoen.2018.04.027

[36] M.H. Abdul-Allah, S.A. Salman, and W.H. Abbas, "Annealing effect on the structural and optical properties of (CuO)(Fe2O3) x thin films obtained by chemical spray pyrolysis," Journal of Thi-Qar Science, **5**(1), 91-96 (2014). https://www.iasj.net/iasj/pdf/a38620e9241bbe5a

[37] A.J. Kadham, D. Hassan, N. Mohammad, and A.H. Ah-Yasari, "Fabrication of (polymer blend-magnesium oxide) nanoparticle and studying their optical properties for optoelectronic applications," Bulletin of Electrical Engineering and Informatics, **7**(1), 28-34 (2018). https://beei.org/index.php/EEI/article/view/839/518

[38] X. Wu, C. Zhou, W.R. Huang, F. Ahr, and F.X. Kärtner, "Temperature dependent refractive index and absorption coefficient of congruent lithium niobate crystals in the terahertz range," Optics express, **23**(23), 29729-29737 (2015). https://doi.org/10.1364/OE.23.029729

[39] M.H. Abdullal, R.A. Jaseen, and A.H. Resan, "Annealing effect on the optical energy gap of (CdTe) thin films," J. Pure Sciences, **7**(3), 205-213 (2011). https://www.iasj.net/iasj/pdf/ccf116d82c221e01

[40] J. Al-Zanganawee, M. Al-Timimi, A. Pantazi, O. Brincoveanu, C. Moise, R. Mesterca, ... & Enachescu, M. "Morphological and optical properties of functionalized SWCNTs: P3OT nanocomposite thin films, prepared by spincoating," Journal of Ovonic Research, **12**(4), 201-207 (2016). https://www.chalcogen.ro/201_AlzanganaweeJ.pdf

[41] A. Manikandan, L.J. Kennedy, M. Bououdina, and J.J. Vijaya, "Synthesis, optical and magnetic properties of pure and Co-doped $ZnFe_2O_4$ nanoparticles by microwave combustion method," Journal of magnetism and magnetic materials, **349**, 249-258 (2014). https://doi.org/10.1016/j.jmmm.2013.09.013

[42] J.M. Rondinelli, and N.A. Spaldin, "Structure and properties of functional oxide thin films: insights from electronic-structure calculations," Advanced materials, **23**(30), 3363-3381 (2011). https://doi.org/10.1002/adma.201101152

[43] S.S.H. Al-Mgrs, M.H. Al-Timimi, M.Z. Abdullah, and W.H. Al-Banda, "Structural and optical characterizations of synthesized CMC/PVP-SnO_2 nano composites," AIP Conference Proceedings, **2475**(1), 090018 (2023). https://doi.org/10.1063/5.0102768

[44] A.J. Mawat, M.H. Al-Timimi, W.H. Albanda, AND M.Z. Abdullah, "Morphological and optical properties of $Mg_{1-x}CdS_x$ nanostructured thin films," AIP Conference Proceedings, **2475**(1), 090019 (2023). https://doi.org/10.1063/5.0103955

[45] Q.M. Jebur, A. Hashim, and M.A. Habeeb, "Structural, electrical and optical properties for (polyvinyl alcohol–polyethylene oxide–magnesium oxide) nanocomposites for optoelectronics applications," Transactions on Electrical and Electronic Materials, **20**(4), 334-343 (2019). https://doi.org/10.1007/s42341-019-00121-x

ПОЛІПШЕННЯ СТРУКТУРНИХ ТА ОПТИЧНИХ ВЛАСТИВОСТЕЙ НАНОСТРУКТУРНИХ ПЛІВОК MgO: SnO_2

Р.Х. Аюб[a], Мухаммад Х. Аль-Тімімі[a], М.З. Абдуллах[b]

[a]*Департамент фізики, науковий коледж, університет Діяла, Ірак*

[b]*Управління досліджень матеріалів, Міністерство науки і технологій, Ірак*

У цьому дослідженні використовується метод хімічного осадження для дослідження структурних і оптичних властивостей наночастинок MgO:SnO_2. Тонкі плівки були нанесені методом центрифугування на скляні підкладки. Рентгеноструктурний аналіз підтвердив кристалічну структуру отриманих тонких плівок з піками, що відповідають площинам (110), (101), (200), (211) і (220), з тетрагональною кристалічною структурою SnO_2. Інфрачервона Фур'є спектрометрія (FTIR) і скануючий електронний мікроскоп (SEM), використовували для характеристики функціональних груп, форми та розмірів синтезованих наночастинок оксиду металу. Оптичні властивості плівок вивчали за допомогою спектроскопії UV-Vis. Енергія забороненої зони була оцінена в діапазоні (3,9-3,4 еВ). Також було визначено показник заломлення та коефіцієнт екстинкції плівок. Результати показали, що плівки мають хорошу прозорість у видимій області. У дослідженні зроблено висновок, що тонкі плівки MgO:SnO_2, технікою покриття методом центрифугування, мають потенційне застосування в оптоелектроніці та у газових датчиках.

Ключові слова: *плівки MgO:SnO_2; техніка спінового покриття; метод осадження; структура; оптичні властивості*